

Cite this: *RSC Adv.*, 2016, 6, 8773

Water soluble stimuli-responsive star copolymers with multiple encapsulation and release properties†

Sandip Das, Dhruba P. Chatterjee,‡ Radhakanta Ghosh, Pradip Das§ and Arun K. Nandi*

A series of three arm star shaped (random/block) and linear water soluble copolymers are synthesised by atom transfer radical polymerization (ATRP) using di(ethylene glycol) methyl ether methacrylate (DEGMA) and 2-(dimethylamino) ethyl methacrylate (DMAEMA). The structure and composition of the block and random copolymers are characterized by ^1H NMR spectra and gel permeation chromatography (GPC). The self-assembly of these copolymers, investigated by dynamic light scattering (DLS), exhibits that below the lower critical solution temperature (LCST) of pDEGMA all the copolymers are soluble in water and possess lower particle size but above its LCST particle size increases particularly in a basic medium. On addition of 8-anilino-1-naphthalenesulfonic acid (ANS) the particle size increases by ~ 10 times below the LCST. Both the DLS and fluorescence studies using a hydrophobic fluorescent dye, exhibit temperature triggered encapsulation and pH triggered release. All the copolymers exhibit highly reversible multiple aggregation at different temperature and pH conditions and require increased temperature for the aggregation with decrease in pH of the medium. The random star copolymer [3-arm-p(DEGMA₄₀-co-DMAEMA₁₈)] exhibits aggregate formation under physiological conditions (37 °C and pH 7.5) and with decreasing the pH to 6.5 the aggregates dissociate. The MTT assay and cell morphology indicate that the three arm star and linear random copolymers have lower cytotoxicity against normal CHO-K1 cells having lower positive zeta potential values.

Received 8th December 2015

Accepted 7th January 2016

DOI: 10.1039/c5ra26144a

www.rsc.org/advances

1. Introduction

Stimuli responsive polymers are extensively studied for their potential applications as 'smart materials',^{1–7} and polymers with the propensity of conformational/polarity change of the entire chain or any of its constituting block, on the influence of any external trigger like temperature,^{2,5} pH,^{2,5,7} light,^{8–13} specific molecules,^{2,14,15} redox^{2,16,17} or its combinations, are classified as stimuli responsive polymers. Water soluble polymers showing stimuli response with temperature and/or pH have received special attention for potential applications in the field of health care and nano-biotechnology.^{18–20} Polymeric systems showing a phase transition of lower critical solution temperature (LCST) or upper critical solution temperature (UCST) types and/or having a block copolymer segment with pH sensitive functional group may function as thermo, pH or thermo-pH dual

responsive systems in aqueous medium. Poly(*N*-isopropylacrylamide) (pNIPAM) is the most studied thermo-responsive water soluble polymer for biological applications having a LCST near the physiological range at around 32 °C (ref. 21 and 22) and the LCST of pNIPAM remains unchanged by slight variation of pH and other chemical environments.^{22–25} Lutz *et al.* have made the application of poly(ethylene glycol) based polymethacrylate systems as a very useful alternative of pNIPAM.^{25–27} Short poly(ethylene glycol) substituted polymer chain, *e.g.* poly[di(ethylene glycol) methyl ether methacrylate] (pDEGMA), exhibits LCST around 21 °C in aqueous solution.^{26,28} However, its LCST may be tuned at higher temperature by copolymerizing with oligo(ethylene glycol) methyl ether methacrylate (OEGMA) in suitable feed ratios of the monomers.²⁹ Similarly, the LCST type phase transition temperatures of a thermo responsive polymer system may also be modified by copolymerization with pH sensitive polymer systems such as *N,N*-dialkyl aminoethyl methacrylates having *N,N* dimethyl or *N,N*-diethyl substituents.^{30,31} In comparison to the pK_a of another basic monomer vinyl pyridine ($\text{pK}_a \sim 4.5$),³² 2-(dimethylamino) ethyl methacrylate (DMAEMA) has a higher pK_a (~ 7),³¹ and therefore pDMAEMA gives the opportunity of reversible protonation and deprotonation of the $-\text{NMe}_2$ groups to have aggregation and disaggregation within the pH window

Polymer Science Unit, Indian Association for the Cultivation of Science, Jadavpur, Kolkata-700 032, India. E-mail: psuakn@iacs.res.in

† Electronic supplementary information (ESI) available: ^1H NMR of TIBB and P₁, GPC, DLS and fluorescence data of P₁, and bar diagram of zeta potential values. See DOI: 10.1039/c5ra26144a

‡ Dept of Chemistry, Presidency University, Kolkata-700 073.

§ Centre for Advanced Materials, IACS, Jadavpur, Kolkata-700 032.

of 5.5 and 7.4, which are typical for malignant tissues and human blood system respectively. Also pDMAEMA shows LCST near 50 °C (ref. 30) at pH = 7, however this is somewhat higher than the normal physiological temperature range of applications therefore in the release or encapsulation mechanism LCST of pDMAEMA would have an insignificant effect.

pDEGMA based polymers offer non-toxicity, anti-immunogenicity and biocompatibility^{25–27} coupled with its facile synthesis technique by ATRP under simple cost effective and environmentally benign conditions.^{33–35} pDEGMA shows LCST-type phase transition in aqueous solution due to the differential solvation of water soluble di(ethylene glycol) moieties and water insoluble polymethacrylate backbone segment. At a temperature lower than 21 °C solvation of di(ethylene glycol) segment is sufficient to keep it soluble in water and above it de-solvation causes aggregation of the chains resulting insolubility of the polymer. Therefore, copolymer of pDEGMA with some other water soluble polymer, having both block and random architecture, may offer a micellar system in aqueous solution above LCST of pDEGMA.

In many applications, reversible dissociation/micellization transitions triggered by external stimuli are desired, as the reformation of micelles allows the re-encapsulation of the released substances.^{8,12} Jiang and Zhao developed dual responsive water soluble block copolymer [poly(ethyleneoxide-*b*-p(DEGMA-co-methacrylic acid))] using thermo and pH sensitive component blocks showing multiple micellization and dissociation transition by coupled application of both of the triggers.³⁴ The carboxylic acid groups of polymethacrylic acid has been used as pH sensitive block and increasing pH of the medium helps in the process of micellar dissociation whereas increased temperature causes remicellization.

So copolymers with pDEGMA as hydrophobic core in aqueous solution may be designed for encapsulation and release of hydrophobic dye molecules. In order to use these micelles for delivery and diagnostic purposes, they must remain in the aggregated state at physiological temperature (37 °C) and at typical blood pH (7.4) followed by its dissociation at the environment of malignant tumour tissues having pH at the acidic range (pH 5.5–6.5).³⁶ Therefore, pDEGMA based copolymers having another component of basic functionalities would be prospective for such application. In order to develop polymeric micelle based carrier systems, the polymer molecules used should have appreciably lower value of critical aggregation concentration (CAC) such that during application, micellar aggregate remains intact irrespective of dilution. In this regard multi-arm polymer systems are more acceptable than linear polymer molecules having comparable molar mass or molar ratios.³⁷ In addition, these multi-arm or branched polymer systems are further attractive than linear polymeric systems due to their lower values of viscosity owing to the lower value of exponent (α) in Mark–Howink–Sakurada equation.³⁸

Here we report the synthesis of 3-arm star shaped random & block copolymers and linear copolymer of pDEGMA and pDMAEMA and compare its multistep micellar aggregation at varied temperature and pH conditions. All these systems require increased temperature for aggregation and subsequent

solubilisation of the aggregate is made by lowering the pH of the medium to a small extent. We have been able to optimize a composition for the 3-arm star random copolymer exhibiting aggregation at pH 7 under physiological temperature and when pH is lowered to a value similar to malignant cells dissociation of aggregate occurs. We have efficiently monitored these changes using a fluorescent dye 8-anilino-1-naphthalenesulfonic acid (ANS) by both dynamic light scattering (DLS) and fluorescence methods with appreciable reversibility. Another hydrophobic dye, Nile red is also encapsulated by the three arm star copolymer and has been monitored through fluorescence spectroscopy. The cell viability and biocompatibility of the copolymers are investigated and possible reason for the relative cell viability has been discussed from the zeta potential values.

2. Experimental section

2.1. Materials and purification

The monomers di(ethylene glycol) methyl ether methacrylate (DEGMA) and 2-(dimethylamino) ethyl methacrylate (DMAEMA) (Aldrich, USA) were purified by passing through a neutral and basic alumina column, respectively. The ligands 1,1,4,7,10,10-hexamethyl triethylene tetramine (HMTETA) and 4,4'-dimethyl-2,2'-dipyridyl (DMDP) (Aldrich, USA) were used as received. Phloroglucinol dehydrate, 8-anilino-1-naphthalenesulfonic acid (ANS) and the initiator 2-bromoisobutyryl bromide (2BIB) (Aldrich, USA) were used as received. The catalyst cuprous chloride (CuCl) (Loba Chemicals, Mumbai) was purified under nitrogen atmosphere by washing with 10% HCl followed by CH₃OH and diethyl ether in a Schlenk tube. The solvents, anisole, chloroform (CHCl₃), dichloromethane (DCM) and tetrahydrofuran (THF) were purchased from Loba Chemicals, Mumbai and were purified by distillation.

2.2. Synthesis

2.2.1. Preparation of 1,3,5-tri(2-bromo-isobutyryloxy)benzene (TIBB). Under nitrogen atmosphere phloroglucinol dehydrate (2 g, 12.3 mmol) and triethylamine (5.1 ml, 32.9 mmol) (Et₃N) were dissolved in 200 ml anhydrous THF at 0 °C. 2BIB (5.25 ml, 42.5 mmol) was then injected drop wise into the reaction vessel and the reaction mixture was then allowed to stand for 24 h. After solvent evaporation by rotary evaporator the dried sample was collected and dissolved in 60 ml ethyl acetate. The reaction mixture was then consecutively washed with water and saturated sodium bicarbonate solution. The organic layer was then separated and was passed through the anhydrous Na₂SO₄ followed by solvent evaporation and re-crystallization at very low temperature to obtain a white crystalline solid as a final product (yield 80%).³⁹

¹H NMR (CDCl₃): δ = 6.95 (3H, s), 2.1 (18H, s); ¹³C NMR (CDCl₃) δ = 169.6, 151.5, 112.6, 54.9 and 30.7.

2.2.2. Preparation of 1,2-bis(bromoisobutyryloxy)ethane (EGBIB). Under nitrogen atmosphere 1.5 ml ethylene glycol was dissolved in 55 ml anhydrous DCM and then 10 ml Et₃N was added into the reaction mixture. 10 ml 2BIB was injected drop

wise into the reaction vessel at 0 °C. The reaction mixture, stirred for overnight, was filtered and was washed with saturated sodium bicarbonate and NaCl solution, respectively. The organic layer was collected, passed through anhydrous Na₂SO₄ and was evaporated by rotary evaporator. The residue was dissolved in methanol at 50 °C and was re-crystallized at -5 °C to obtain white needle like crystal of the product (yield 75%).⁴⁰

¹H NMR (CDCl₃): δ = 1.95 (12H, s), 4.45 (4H, s); ¹³C NMR (CDCl₃) δ = 172, 63, 54.5 and 30.5.

2.2.3. Synthesis of 3-arm-poly[di(ethylene glycol) methyl ether methacrylate]₃-Cl₃ macro-initiator {3-arm-p(DEGMA)₃-Cl₃}. 30 mg TIBB, 2 ml anisole, 5 mg CuCl were taken in a nitrogen purged reaction vessel (8 × 2.5 cm) and DEGMA (1 ml) was injected into the reaction vessel under nitrogen atmosphere. Then 16 mg DMDP was added into the reaction vessel and the closed reaction vessel was then kept at 55 °C for 10 h under stirring condition. The reaction mixture was poured into excess petroleum ether (boiling range 60–80 °C) and the separated polymer was isolated, re-dissolved in THF and was re-precipitated into excess petroleum ether. The process was repeated for three times to remove any trace amount of monomer entrapped within the polymer. Then the THF solution of the polymer was passed through silica column to remove copper and was followed by solvent evaporation to obtain the polymer (Scheme 1) (yield-70%).

2.2.4. Synthesis of 3-arm-poly[di(ethylene glycol) methyl ether methacrylate]-block-poly[2-(dimethylamino) ethyl methacrylate] {3-arm-p(DEGMA₃₄-B-DMAEMA₂₁)} (P₁). In another nitrogen purged reaction tube 0.6 g 3-arm-p(DEGMA)₃-Cl₃, 1 ml anisole, 5 mg CuCl were taken and the monomer DMAEMA (1 ml) was injected and nitrogen purging was continued for 20 min. The reaction tube was closed with a rubber septum and 10 μL HMTETA was injected, stirred for 10 h at 50 °C, and was precipitated into excess petroleum ether (60–80 °C). The polymer was separated, re-precipitated from THF with excess petroleum ether. The trace amount of monomer entrapped within the polymer was removed by repeated dissolution and re-precipitation. The polymer was finally dissolved in THF, passed through silica column, followed by solvent evaporation to obtain copper free 3-arm-p(DEGMA₃₄-B-DMAEMA₂₁) (Scheme 1, yield-40%). From the NMR data the mole ratio of DEGMA (62%) and DMAEMA (38%) are observed in the 3-arm star block copolymer.

2.2.5. Synthesis of 3-arm random poly[di(ethylene glycol) methyl ether methacrylate]-co-poly[2-(dimethylamino) ethyl methacrylate] copolymer {3-arm-p(DEGMA_r-R-DMAEMA_i)}. 30 mg TIBB, 3 ml anisole and 10 mg CuCl were taken in nitrogen purged similar reaction vessel. The monomers DEGMA and DMAEMA were next injected and nitrogen purging was continued for 25 min. For the synthesis of different random copolymers 3-arm-p(DEGMA₃₃-R-DMAEMA₂₃) (P₂), 3-arm-p(DEGMA₄₀-R-DMAEMA₁₈) (P₃) and 3-arm-p(DEGMA₁₆-R-DMAEMA₃₅) (P₄), the two monomers DEGMA and DMAEMA were taken in 3 : 2, 2 : 1 & 1 : 2 (v/v) ratios (mole ratios are 60 : 40; 66 : 33; 33 : 66) respectively. The reaction vessel was then closed with a rubber septum and 40 μL HMTETA was injected and was sealed with para film followed by stirring for

18 h at 30 °C. After the desired time the reaction mixture was precipitated into excess petroleum ether (60–80 °C) and the resultant polymer was separated, re-dissolved in THF and was re-precipitated with petroleum ether for repeated times to eliminate the small amount of entrapped monomer. To remove copper the THF solution of the polymer was then passed through silica column and was followed by solvent evaporation to obtain pure polymer (yield-70%).

2.2.6. Synthesis of linear-random poly[di(ethylene glycol) methyl ether methacrylate]-co-poly[2-(dimethylamino) ethyl methacrylate] copolymer {L-p(DEGMA₃₂-R-DMAEMA₂₃)}. Also the linear copolymer L-p(DEGMA₃₂-R-DMAEMA₂₃) (P₅) is synthesized by ATRP using EGBIB as the initiator and CuCl/HMTETA (catalyst/ligand) system at 25 °C. The mole ratio of DEGMEM and DMAEMA are taken as 60 : 40.

2.3. Characterization techniques of the polymers

2.3.1. ¹H NMR spectra. The ¹H NMR and ¹³C NMR spectra were recorded in CDCl₃ with a 500 MHz Bruker NMR spectrometer.

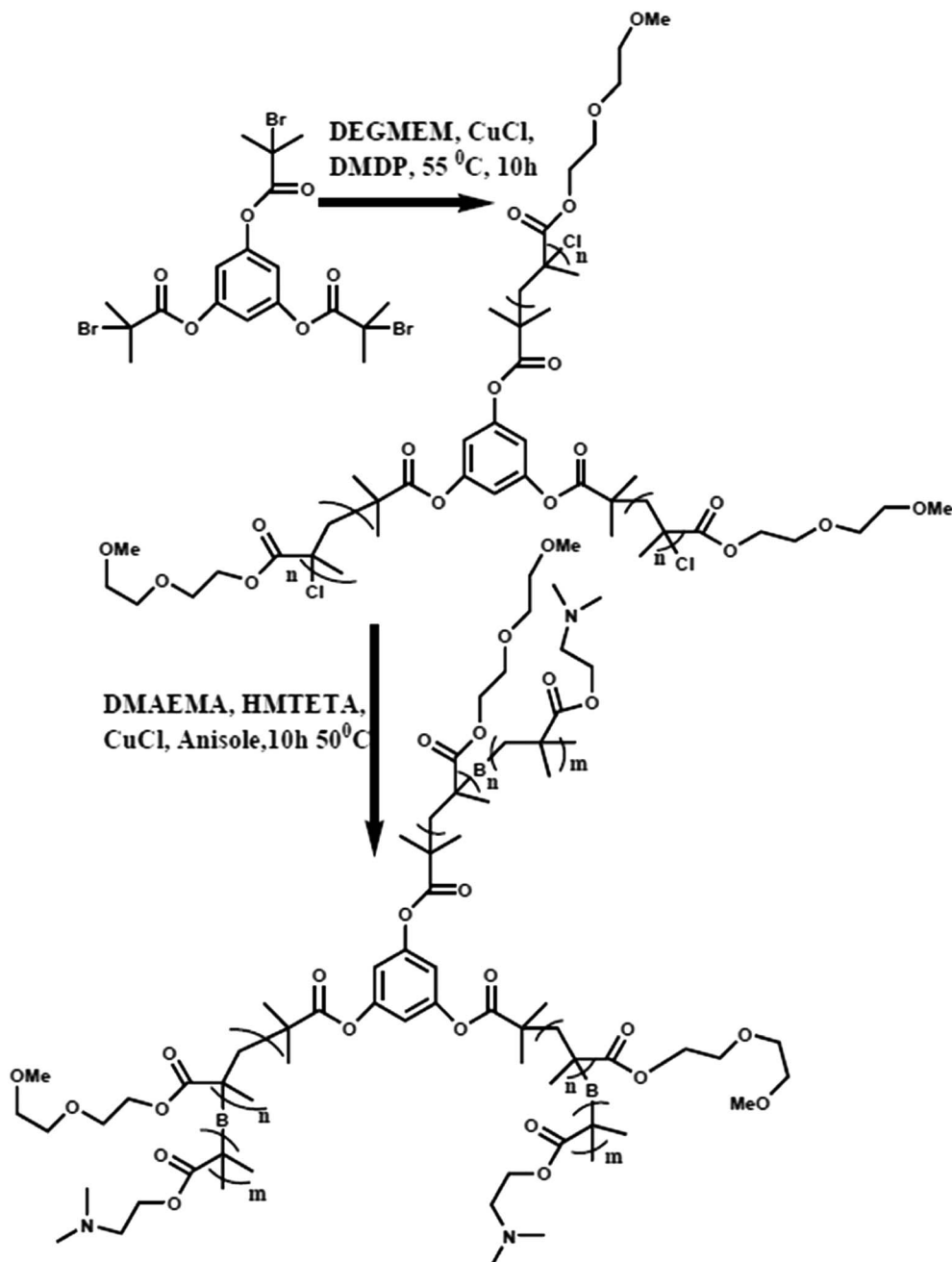
2.3.2. Gel permeation chromatography. The gel permeation chromatography (GPC) experiments were performed on a Waters instrument equipped with Waters 1515 pump, Waters 2414 differential refractive index detector and three μ-styragel column using poly(methyl methacrylate) (pMMA) as the standard and dimethylformamide (DMF) as the solvent.

2.3.3. TEM microscopy. The morphology of the P₃ copolymer samples (with and without ANS) were monitored by transmission electron microscopy (TEM JEOL, 2010EX) operated at an acceleration voltage of 200 kV and fitted with a CCD camera. A specimen for TEM study was made by spreading a small drop of the above transparent solution on a carbon-coated copper grid and allowing the drops to dry in air at low temperature (5 °C) and finally in vacuum at 30 °C for about 1 day. Another TEM grid is also prepared by drying the TEM grids at high temperature (above LCST, 40 °C).

2.4. Instrumental techniques

2.4.1. Dynamic light scattering (DLS). The DLS experiments were performed using a Malvern instrument with a He-Ne laser at an angle 173°. For temperature dependent experiment, the aqueous solution of the polymer was heated from low to higher temperature. After reaching the desired temperature the sample was allowed to equilibrate at that temperature for 5 min before both the heating and cooling experiments. The zeta potential value of the aqueous solution of the copolymers [1 mg ml⁻¹; 0.1% (w/v)] were measured using the same DLS instrument at 25 °C.

2.4.2. Fluorescence study. The temperature dependent photoluminescence (PL) spectra of all the copolymer solutions (0.4% w/v) containing 17 μM ANS probe were recorded using a Fluoromax-3 (Horiva Jovin Yvon) instrument. The sample was taken in a quartz cell with 1 cm path length and was excited at 370 nm. Emission scans were recorded from 390 to 620 nm using a slit width of 3 nm with an increment of 1 nm wavelength having an integration time of 0.1 s. Samples were permitted to



Scheme 1 Synthetic procedure adopted for the preparation of 3-arm-p(DEGMA)₃-Cl₃ macro-initiator and P₁ copolymer (B means block copolymer).

stand for 10 minute at each temperature for equilibrating the temperature.

2.5. Measurement of pK_a values

pK_a values of the different copolymers were measured by acid-base titration method from 0.3% (w/v) solutions of the polymers using pH meter (Oakton).

2.6. Cytotoxicity

The effect of different copolymer on normal cells morphology was observed by optical microscope. Chinese hamster ovary

CHO-K1 cells were seeded in 24-well plate in presence of 500 μL Dulbecco's modified Eagle medium (DMEM) medium supplemented with 10% fetal bovine serum (FBS) and 1% penicillin/streptomycin at 37 °C and 5% CO₂. After overnight growth, the cells were incubated with different polymer at final concentration of 200 μg ml⁻¹ for 24 hours. Then cells were washed with PBS buffer solution to remove the unbound polymer micelle. Then fresh 500 μL of supplemented DMEM medium was added. The cells morphology was observed by using Olympus IX81 optical microscopy.

The cell viability of different copolymer against normal CHO-K1 cells was evaluated by conventional 3-(4,5-dimethylthiazol-2-

yl)-2,5-diphenyltetrazolium bromide (MTT) assays. The cells were seeded in 24-well plates at high density in 500 μL of DMEM medium supplemented with 10% FBS and 1% penicillin/streptomycin at 37 $^{\circ}\text{C}$ and 5% CO_2 . After overnight of cell attachment, the cells were incubated with different copolymer at final concentrations (10–200 $\mu\text{g mL}^{-1}$ and upto 1 mg mL^{-1} only for P_3 copolymer) for 24 hours. Then cells were washed with PBS buffer solution and fresh 500 μL of supplemented DMEM medium were added to each well. After that 50 μL of aqueous solution of MTT (5 mg mL^{-1}) were added and allowed to stand for 4 hours. The violet formazan was dissolved in 500 μL of sodium dodecyl sulfate solution in water/DMF mixture. Absorbance of formazan solution was measured at 570 nm using a BioTek SynergyMx microplate reader.

3. Results and discussion

3.1. Synthesis and characterization

Thermo and pH responsive linear, 3-arm star shaped block and random co-polymeric (pDEGMA-*B/R*-pDMAEMA) systems are synthesized by ATRP technique under amiable conditions. Synthesis of linear and star shaped pDEGMA-co-pDMAEMA [p(DEGMA-*R/B*-DMAEMA)] polymer systems is conducted using EGBIB and 1,3,5-tri(2'-bromo-isobutyryloxy) benzene (TIBB) as initiators, respectively. For the synthesis of three arm star shaped P_1 block copolymers, at first 3-arm-p(DEGMA) $_3$ -Cl $_3$ is synthesized with CuCl/DMDP catalyst at 55 $^{\circ}\text{C}$ and in subsequent step, polymerization of DMAEMA is made using the above macro-initiator with CuCl/HMTETA catalyst/ligand system at 50 $^{\circ}\text{C}$ in anisole (Scheme 1) and the macroinitiator 3-arm-p(DEGMA) $_3$ -Cl $_3$ is produced instead of 3-arm-p(DEGMA) $_3$ -Br $_3$ due to halogen exchange.⁴¹ Also the linear copolymer L-p(DEGMA $_{32}$ -*R*-DMAEMA $_{23}$) (P_5) is synthesized by ATRP using CuCl/HMTETA (catalyst/ligand) system at 25 $^{\circ}\text{C}$ (Scheme 2).

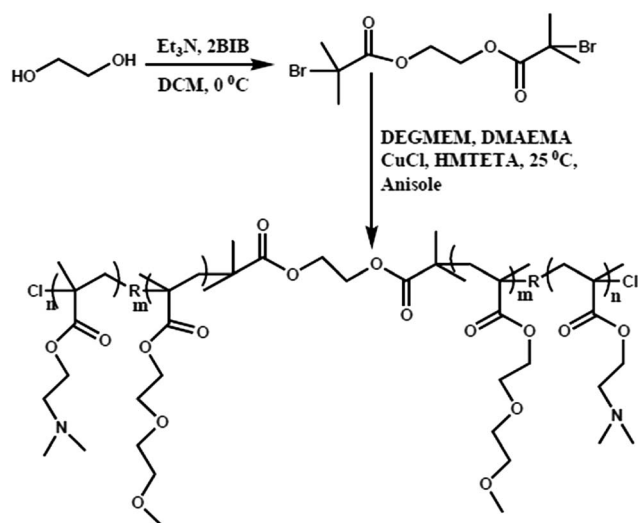
The ^1H NMR spectrum of P_2 copolymer (Fig. 1) exhibits all the characteristic signals of pDEGMA and pDMAEMA segments

present in the polymer. Signals at the δ values 0.8–1.1 ppm and 1.7–2.0 ppm are due to 't' and 'r' protons, respectively and splitting is observed for different tacticities of the methacrylate polymer chains. Protons 'j', 'i', and 'h' present in pDMAEMA units resonate at δ values 2.25, 2.6, and 4.05 ppm, respectively and the signals at 3.35, (3.55–3.75) and 4.15 ppm corresponds to 'g', 'f', and 'e' protons, respectively, present in the pDEGMA units. It is important to note that signal at about δ values of 7 ppm corresponds to three aromatic ring protons present in the TIBB initiator of the polymer and it is also found in the ^1H NMR spectrum of TIBB (Fig. S1†). Similar ^1H NMR spectrum is observed for P_1 block copolymer (Fig. S2†). The NMR spectrum of P_5 copolymer is presented in Fig. 2. Mole ratios of DEGMA and DMAEMA monomer units in different copolymeric systems are calculated from the signal area ratios of proton 'g' and 'j' with respect to 'b' and 'b'' protons, respectively.

Fig. S3a† shows gel permeation chromatography (GPC) trace corresponding to 3-arm star shaped random copolymer (P_2) of pDEGMA and pDMAEMA having 59 and 41 mol% of their corresponding monomeric units (Table 1). GPC trace in Fig. S3a† shows a relatively sharp signal but having a small shoulder at the high molecular end of the distribution curve. However, no trailing is observed at the lower molar mass side of the GPC trace, which indicates that the bimolecular termination occurs at the advanced stages of the reaction leading to the generation of high molar mass dead polymers. Fig. S3b† shows the overlay of GPC traces corresponding to the macro initiator 3-arm-p(DEGMA) $_3$ -Cl $_3$ and 3-arm block copolymer (P_1). In Fig. S3b† prominent bimodality is noticed in case of 3-arm-p(DEGMA) $_3$ -Cl $_3$ macro-initiator and also in the P_1 block copolymer. Development of the shoulder at high molar mass side of the GPC traces during P_2 synthesis may be as a result of inefficient deactivation from Cu/HMTETA catalyst.³³ Similar bimodality is also observed during homo polymerization of DEGMA with bipyridyl based copper catalyst in anisole medium. This may be further attributed to the lesser activity of Cu/bpy complex in polar aprotic medium than in polar protic medium. Also some star-star coupling product is inevitable during this type of radical polymerization.⁴²

3.2. Phase separation

In Fig. 3 the plots of Z-average sizes of the polymers P_2 , P_3 and P_5 obtained from DLS study at different pH of the medium are presented. It is evident from the plots that all the polymers exhibit small size (~ 30 nm) at lower temperatures probably due to the micelle formation as pDEGMA segments are hydrophobic and pDMAEMA is hydrophilic in nature producing a self organized micellar structure with former segments at the core. But after attaining a certain temperature increase of size occurs particularly for pH 9.2. The onset temperature of increase of size may be called as LCST-type phase transition temperature of the respective polymers and it arises due to breaking of H-bonding interactions between pDEGMA segments of the copolymers with the water molecules causing aggregation of the co-polymer chains. But pDMAEMA chains (LCST ~ 50 $^{\circ}\text{C}$) though tend to remain soluble become entrapped within the aggregate of



Scheme 2 Synthetic procedure adopted for the preparation of the linear P_5 copolymer (R means random copolymer).

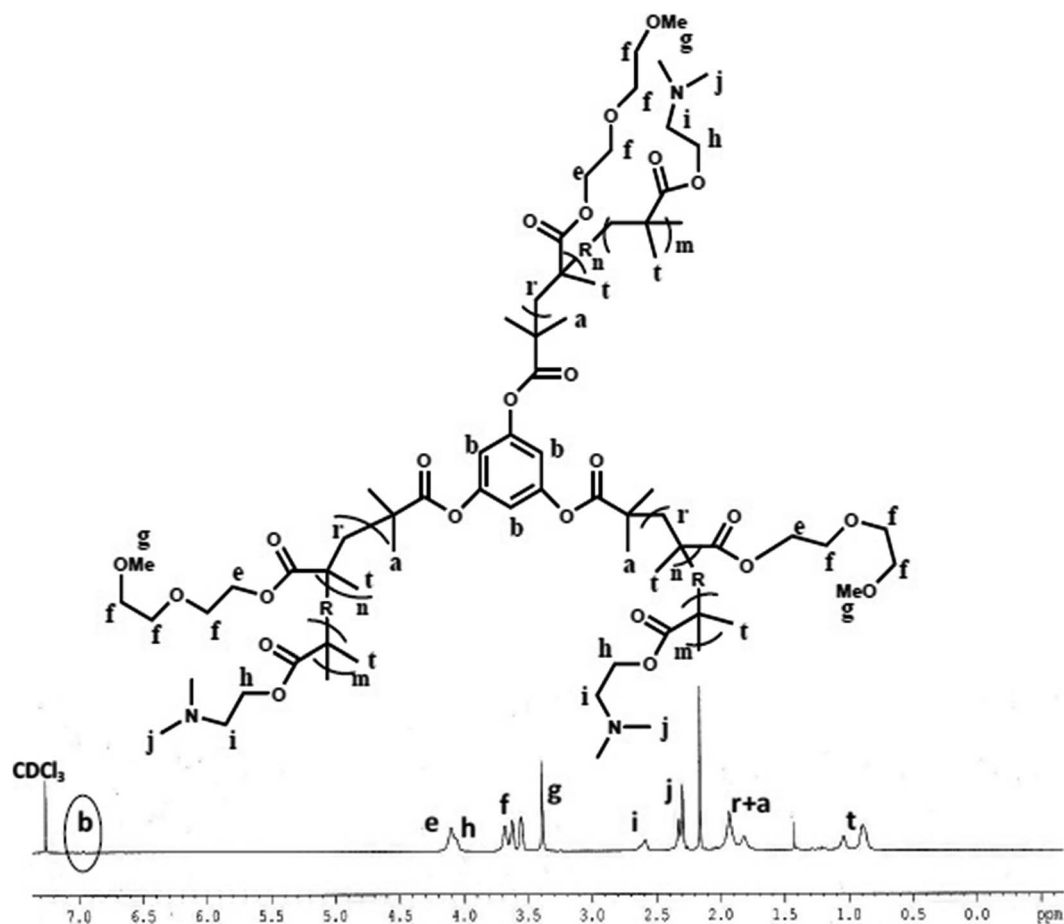


Fig. 1 ^1H NMR spectrum of P_2 copolymer in CDCl_3 along with their peak assignments.

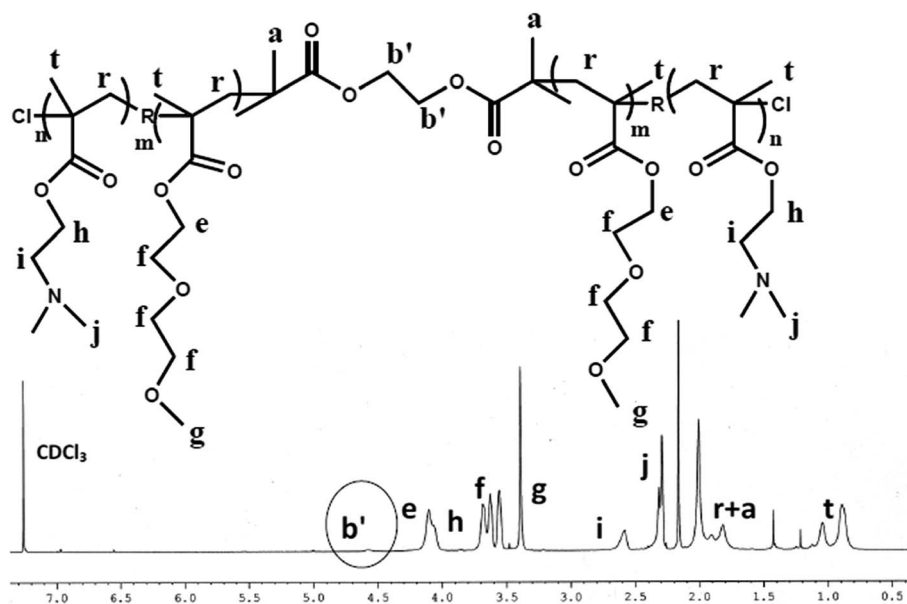


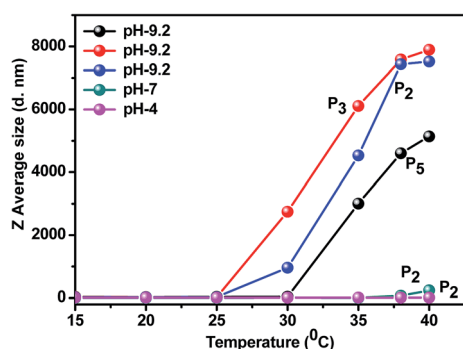
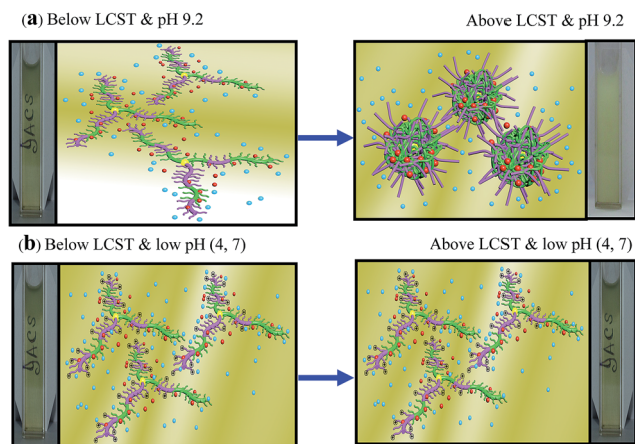
Fig. 2 ^1H NMR spectrum of P_5 copolymer in CDCl_3 along with their peak assignments.

pDEGMA part. This causes an increase of the Z-average size with rise of temperature above the LCST. However, this type of increase of size is not observed at pH 7 and 4 and it has been

attributed to the solvated nature of the copolymers in these pH values because the protonation of basic $-\text{NMe}_2$ group ($\text{pK}_a \sim 7$)^{31,43} causes increased solubility (Scheme 3b). The pK_a values

Table 1 Compositions of the various constituents present in the synthesized star and linear copolymers

Polymer	Entry	Monomer feed ratio used		Molar ratio obtained from ^1H NMR		Molar mass from GPC (Da)	Dispersity	Molar mass from ^1H NMR (Da)	No. of DEGMA & DMAEMA unit per arm
		DMAEMA (mol%)	DEGMA (mol%)	DMAEMA (mol%)	DEGMA (mol%)				
3-arm-p(DEGMA ₃₄ -B-DMAEMA ₂₁)	P ₁			38	62	25 500	1.19	30 000	34 & 21
3-arm-p(DEGMA ₃₃ -R-DMAEMA ₂₃)	P ₂	40	60	41	59	28 300	1.26	30 100	33 & 23
3-arm-p(DEGMA ₄₀ -R-DMAEMA ₁₈)	P ₃	33	66	36	63	26 700	1.23	31 300	40 & 18
3-arm-p(DEGMA ₁₆ -R-DMAEMA ₃₅)	P ₄	66	33	69	30	21 900	1.25	26 500	16 & 35
L-p(DEGMA ₃₂ -R-DMAEMA ₂₃)	P ₅	40	60	39	61	15 100	1.28	19 700	32 & 23

Fig. 3 Z average size vs. temperature plot of P₂, P₃, and P₅ copolymer in aqueous medium (0.4% w/v) at different pH.

Scheme 3 (a) Schematic illustration of change in hydrated structure of P₂ copolymer above LCST of pDEGMA chain at pH 9.2. (b) Schematic illustration of change in hydrated structure of P₂ copolymer above LCST at low pH (4 & 7). [Sky colour spheres stand for water molecules, green hairs correspond to pDEGMA chain, violet hairs stand for pDMAEMA chain and red spheres represents ANS molecule. The green shell surrounding the yellow sphere represents the collapsed structure of pDEGMA chain above its LCST].

determined from titrimetric method of the copolymers P₁, P₃, P₄, and P₅ are 6.29, 6.30, 6.31 and 6.40, respectively. At lower pH the $-\text{NMe}_2$ groups become protonated and columbic repulsion between the $-\text{NMe}_2\text{H}^+$ groups prevent the precipitation of pDEGMA chain even at higher temperatures. A comparison of

the onset temperatures of P₂ and P₅ systems, having similar chain composition but differing in architecture, indicates that the 3-arm random copolymer has lower LCST phase transition than that in the linear copolymer.

Fig. 4 shows the DLS study of 3-arm random copolymer (P₂) in aqueous medium in the presence of ANS molecule with variation of temperature in different pH values. In Fig. 4a it is observed that below 26 °C relatively bigger sized particles (~400 nm) than that in pure P₂ is noticed at pH-9.2. No definite reason for the large size of the copolymer – ANS system below 26 °C is known and it may be attributed to the hydrophobic ANS molecules, some of which may remain entrapped at the pDEGMA core of the copolymer micelle. Even the possibility of increasing multiple chain aggregation of the copolymer *via* supramolecular interaction with the ANS molecule is inevitable. Upon increasing temperature, above 26 °C, the particles size of the polymer shows a similar significant hike which is attributed to the fact that at this pH above 26 °C LCST of pDEGMA segment is reached. Hence, pDEGMA chains become insoluble in water producing large aggregated structures (Scheme 3a). At lower pH (4 & 7) on increase of temperature no sharp increase of hydrodynamic size is noticed (Fig. 3a) due to the solvated nature of pDMAEMA chains as discussed above.

Fig. 4b shows a thermo-reversible nature of the formation and dissociation of the aggregates at pH 9.2 as similar variation of particle size is noticed during both heating and cooling processes. The same behaviour is observed during DLS analysis of P₁ system (Fig. S4†) which also has almost similar mole ratio (Table 1) of DEGMA and DMAEMA units of P₂. A keen observation of the phase transition data indicates that P₁ solution has 2 °C lower transition temperature than that of P₂ solution at pH 9.2. It alerts us the architectural dependency of hydrophobic/hydrophilic moiety among the random and block structures of the 3-arm star copolymer. The block structure favour aggregation at lower temperature than the random one causing a lowering of LCST. This is because the randomly distributed segments of DEGMA remain soluble due to the better influence of statistically distributed DMAEMA segments. But in case of P₁ block copolymer this effect is less and pDEGMA block gets aggregated more easily showing lower LCST.

Fig. 5a shows the TEM images of P₃ dried from its aqueous solution at 5 °C which is below the LCST of pDEGMA at pH 9.2. As expected, below the LCST of pDEGMA, the TEM image

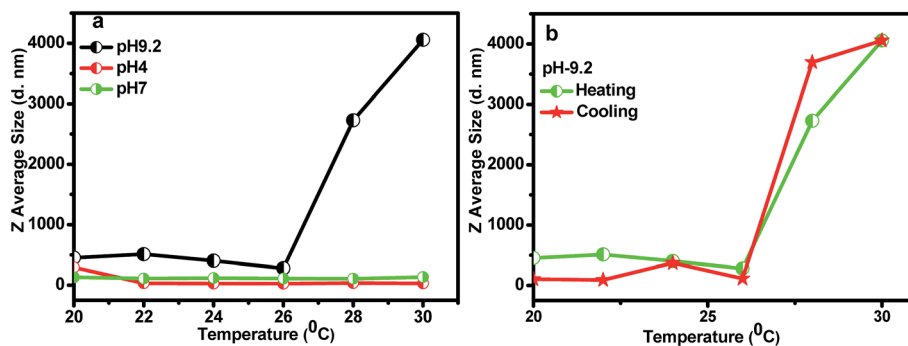


Fig. 4 (a) Z average size vs. temperature plot of P_2 copolymer containing $17 \mu\text{M}$ ANS at different pH obtained from DLS study in aqueous solution (0.4% w/v) and (b) Z average size vs. temperature plot of P_2 (0.4% w/v) containing $17 \mu\text{M}$ ANS at pH-9.2 with increasing and decreasing of temperature.

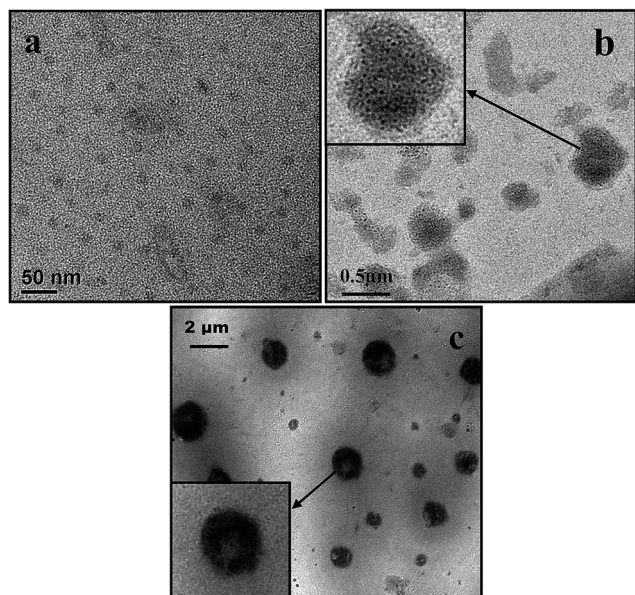


Fig. 5 TEM images of P_3 copolymer at (a) low temperature (below LCST) without ANS (b) low temperature (below LCST) with ANS (c) higher temperature (above LCST) with ANS.

(Fig. 5a) exhibit homogeneously distributed micellar morphology. The TEM grid produced from the same P_3 sample with $17 \mu\text{M}$ ANS probe exhibit bigger size ($\sim 400 \text{ nm}$) and from the inset picture small black spots, possibly of aggregated ANS particles, are noticed inside the structure (Fig. 5b, inset). The ~ 10 times increase of size in the presence of ANS is interesting and may be attributed to the ANS induced aggregation of P_3 chains through noncovalent interaction. But TEM grid dried at 40°C (above the LCST) exhibits a very large aggregated structure ($\sim 2 \mu\text{m}$) produced from the LCST type phase separation of self organized pDEGMA chains inducing the majority of pDMAEMA chains to precipitate due to entrapment. The larger aggregates are produced from the aggregation of small aggregates and a careful observation indicates a vesicular like structure (inset Fig. 5c). Possibly above LCST during the collapsing of micellar aggregates the pDMAEMA segments of the three arm structure of the polymer do not fully collapse and the outer remaining

segments facilitate to entrap water molecules at the centre. This results in the formation vesicular aggregates showing a very large dimension above the LCST.

The P_3 solution has self-assembled pDEGMA chains at the core and hydrophilic corona having dispersed pDMAEMA chains producing micellar structure in the solution. This may be evidenced from the observation of increasing fluorescence intensity of the fluorescent probe (ANS) which itself exhibits almost a non-detectable fluorescence in aqueous solution but in the P_3 solution it exhibits ~ 3 times higher fluorescence intensity (Fig. S5†) for its partial encapsulation at the hydrophobic core of the micelle. The critical aggregation concentration (CAC) of P_3 and P_5 with $17 \mu\text{M}$ ANS solution can also be obtained from this method. Fig. 6a and b shows that 3-arm star polymeric system (P_3) in aqueous solution has shown a CAC value of 0.2 mg ml^{-1} , whereas the CAC value of linear P_5 polymer is $0.53 \text{ mg m}^{-1} \text{ L}^{-1}$ at 45°C . This result indicates that the P_3 has lower CAC value than that of P_5 both having comparable mole ratios of the co-monomers. This gives us indirect evidence that P_3 produced is a three arm star copolymers which usually exhibit lower CAC values due to lower viscosity than that of the linear copolymer.³⁸

Fig. S6a† shows the increase of fluorescence intensity of aqueous solution of $17 \mu\text{M}$ ANS solution taken in the presence of 0.4% (w/v) P_2 solution with increasing temperature. This increase in fluorescence intensity of ANS at and above 26°C indicates greater degree of solvation of ANS from the water molecules within the hydrophobic core of the polymer aggregate. Therefore, it may be argued that above LCST of pDEGMA, this aggregated structure may act as better scaffolds for encapsulating hydrophobic molecules like dyes, drugs and other organic pollutants. The fluorescence intensities for both heating and cooling process of P_2 (Fig. 7a) when plotted with temperature exhibits high degree of reversibility. The reversibility also indicates that such release and recapturing of hydrophobic ANS molecule at the core by pDEGMA units would occur very efficiently with decrease and increase of temperature, respectively. Another hydrophobic dye Nile red also exhibits similar increase of fluorescence intensity due to encapsulation of the dye within the hydrophobic core of the P_3 due to increase of temperature (Fig. S6b† and 7b).

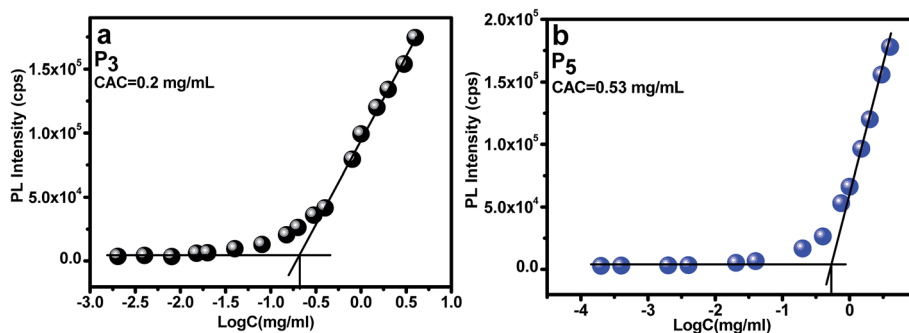


Fig. 6 PL intensity vs. $\log(C)$ plot for (a) P_3 and (b) P_5 copolymers where C indicates concentration of polymer solution at 45°C .

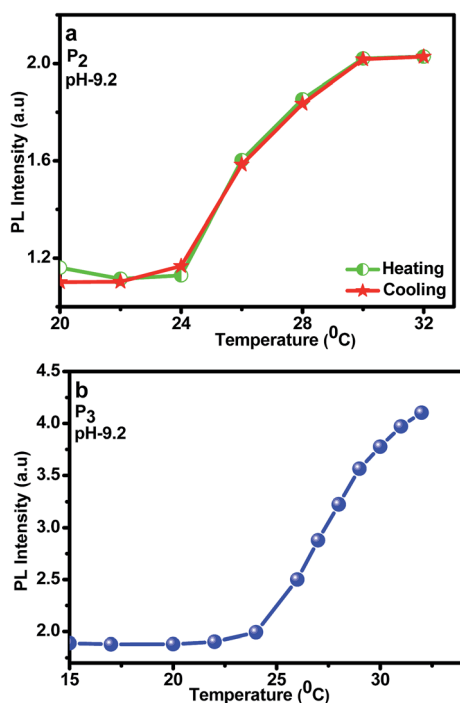


Fig. 7 (a) PL intensity vs. temperature plot of P_2 copolymer solution (0.4% w/v) containing $17\ \mu\text{M}$ ANS with increasing temperature at pH-9.2. (b) PL intensity vs. temperature plot of P_3 copolymer solution (0.4% w/v) containing $17\ \mu\text{M}$ Nile red at pH-9.2 with increasing temperature.

Fig. S7a and b† exhibits the fluorescence data with temperature for both heating and cooling processes of aqueous solution of P_1 copolymer with same quantity of ANS probe. Evidently, in this case the reversibility is relatively poor in spite of having almost similar mole ratio of pDEGMA and pDMAEMA units with P_2 . This may be due to the well segregated nature of pDEGMA and pDMAEMA in this block copolymer than their random counterpart. The presence of randomly distributed hydrophilic pDMAEMA segments helps the pDEGMA chains to attain the reversibility better than that of the block co-polymer in encapsulating and releasing of ANS probe. This is because the randomly distributed pDMAEMA chains within pDEGMA domains entrap some water molecules (being associated with pDMAEMA chains) within the pDEGMA domains above its LCST. It is unlike the block copolymer systems where under

similar conditions they remain in well segregated state. It is interesting to note that during cooling below the LCST the fluorescence intensity of ANS crosses that of the heating curve and exhibits much lower value than that at the onset of heating. A probable reason is that at the onset of heating the polymer chains remain somewhat H-bonded with each other and with water molecules, but during instant cooling due to the lack of sufficient time for equilibration the inter-chain H-bonding is much lesser, causing the ANS molecules more free exhibiting lower fluorescence intensity.²⁷ Fig. S7a† shows that in case of P_1 copolymer the fluorescence hike has started from 22°C but in case of DLS study the increase of particle size occurs at 24°C . Both the increase of particle size and increase of fluorescence intensities of the ANS probe are indicative of starting of molecular aggregation. However, the light scattering technique requires some critical degree of aggregation prior being detected, hence DLS result shows LCST phase transition at higher temperature than that found in fluorescence study arising from the decrease of local polarity around ANS molecules as soon as pDEGMA chains start getting dehydrated with increase in temperature.

3.3. Multiple aggregation & release of hydrophobic molecule

The DLS data of 3-arm-p(DEGMA₁-R-DMAEMA₂) having $17\ \mu\text{M}$ ANS solution exhibit the phenomenon of multiple aggregation with variation of temperature and pH (Fig. 8). The P_2 system shows increase in particle size due to aggregation at 27°C when the medium pH is 9.2 (Fig. 8a). At this condition when $33\ \mu\text{L}$ of 1 (M) HCl solution is added, suddenly the pH drops to 8.5 and immediate dissociation of the micelles occurs causing the particle size to drop to a lower value similar to that at 24°C of pH 9.2.

At this pH value of 8.5, when the system is further heated aggregate formation again starts and maximum increase of size occurs at about 34°C . This once more changes by lowering the pH of the medium to 7.5 by the addition of $20\ \mu\text{L}$ 1 (M) HCl and it returns almost to the molecularly dissolved state of the polymer. On further heating, this system again exhibits aggregation showing a maximum size at 43°C . Addition of $10\ \mu\text{L}$ 1 (M) HCl decreases the medium pH from 7.5 to 6.5 and the aggregates further dissociate. Evidently at a particular pH value, the incidence of aggregate formation results from the

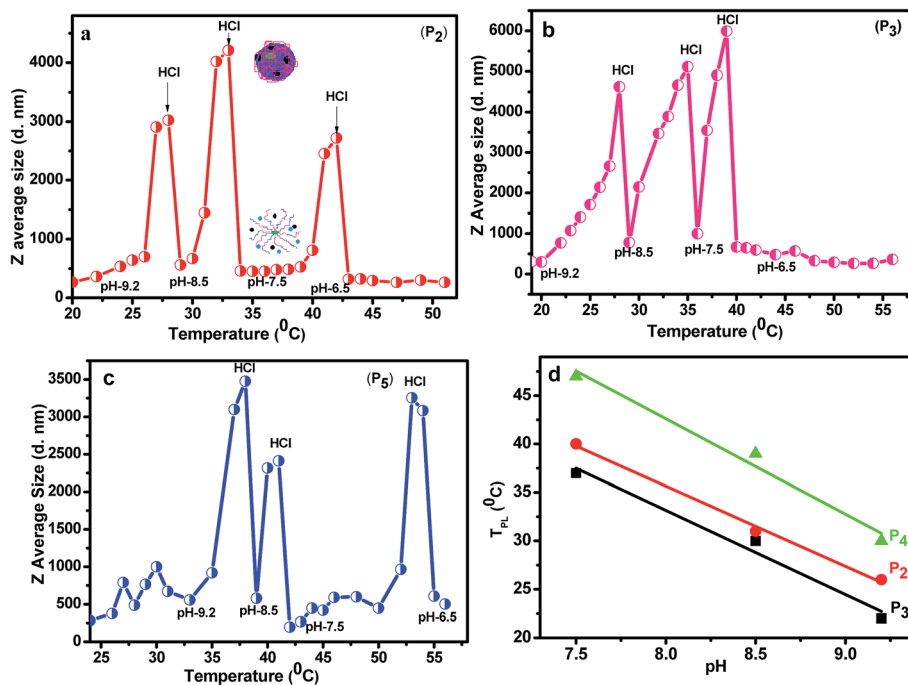


Fig. 8 (a) Z average size vs. temperature plot of aqueous solution of P₂ (b) P₃ (c) P₅ copolymers with 17 μ M ANS solution for variation of pH and (d) phase transition temperature (T_{PL}) vs. pH plots of different 3-arm random copolymers.

development of hydrophobicity with increase of temperature causing aggregation of pDEGMA segments. At pH 6.5, protonation occurs at the basic $-NMe_2$ groups developing poly-cations and therefore at that particular temperature precipitation of the pDEGMA chains becomes restricted due to the repulsion between the $-NMe_2H^+$ groups followed by its solvation and the increased solubility of the polymer causes 'aggregate-burst'. Fig. 8a also shows an increase of particle size due to increase in temperature or decrease in particle size due to pH lowering. It occurs almost vertically with respect to the temperature axis indicating that the process of aggregation or dissociation is quite sharp and also very much reversible. Fig. 8b shows the DLS analysis of P₃ system which is slightly richer in pDEGMA than the previous system P₂. This system also shows similar event of multiple aggregation and most important is that it shows aggregate formation in the physiological range of pH-7.5 and temperature $\sim 37^\circ\text{C}$, which may be very much interesting with respect to its application in biological systems. Fig. S8† shows a similar study with P₄ copolymer, a system which is rich in pDMAEMA. A closer look to the DLS analysis of this system reveals that the onset of phase transition temperature of LCST type (T_{PL}) of the copolymer at a given pH gradually increases probably due to the increasing proportion of more hydrophilic pDMAEMA segment. At pH 9.2, P₂, P₃ and P₄ copolymer systems exhibit T_{PL} at 26, 22 and 30°C , respectively. Fig. 8c shows the aggregation and dissociation transitions of the linear P₅ system. This system also has comparable mole ratios of DEGMA and DMAEMA units as in P₁ and P₂ copolymers. Here also three stages of aggregation and dissociation transition are observed at the same temperature range (25–55 $^\circ\text{C}$) and pH range (9.2–6.5). In Fig. 8d the variation of the transition temperature (T_{PL})

of the 3-arm random copolymers with pH are presented and it is evident that the T_{PL} of all the copolymers decreases almost linearly with increase of pH of the medium. It is also important to note that for the 3-arm random copolymer at the same pH the T_{PL} decreases with increase of DEGMA concentration for the increased hydrophobicity.

Fig. 9 shows the variation in fluorescence intensity of ANS in P₂ copolymer solution under varied temperature and pH conditions. At pH 9.2 when the temperature of the system is raised, maximum fluorescence intensity signifying maximum amount of ANS encapsulation occurs at about 30°C and as soon as pH of the system is lowered to 8.5 by addition of HCl, fluorescence intensity gets reduced to the initial value of molecularly dissolved state. This result signifies the release of ANS molecules from the hydrophobic core of the aggregate following a 'aggregate-burst'.

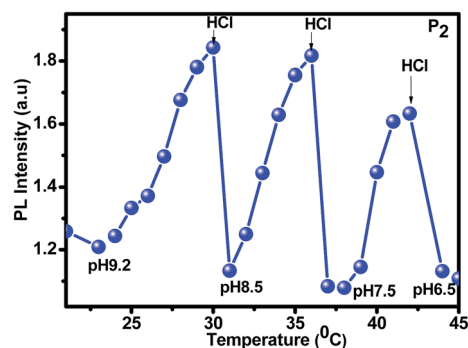


Fig. 9 Fluorescence intensity vs. temperature plot of aqueous solution of P₂ copolymer containing ANS probe with variation of pH.

The similar sequence of ANS entrapment within the aggregate core with increasing the temperature occurs at pH 8.5 showing maximum intensity at 36 °C and the release of ANS occurs as soon as the pH is lowered to 7.5 by addition of HCl. On further heating at this pH value, maximum extent of ANS encapsulation associated with maximum fluorescence intensity is observed at 42 °C. Therefore, analysis of multiple aggregation of P_2 in aqueous solution using the ANS fluorescence probe shows very much similar result as observed during DLS analysis.

Therefore, the different polymer systems used in this study may be useful for reversible capturing and release of suitable hydrophobic dye or drug molecules depending on the pH and temperature of the system. In this respect P_3 would be very much successful as it shows dye encapsulation at pH 7.5 and at 37 °C both of which are physiologically very much important as 37 °C is normal physiological temperature and blood pH is about 7.4. Therefore, in case of entrapment of any suitable hydrophobic dye/drug molecule, this polymer system should exhibit maximum loading in the range of 37 °C at pH 7.5. This reversible temperature/pH triggered uptake and release of dye molecules might be useful for delivery in biological systems particularly at lower pH.

3.4. Biocompatibility and cell viability

All the copolymers P_1 , P_2 , P_3 and P_5 are temperature sensitive and pH responsive, which are biologically very important parameters to oblige with different biological applications. For this purpose we have made cytotoxicity analysis of all four different types of copolymers separately (Fig. 10a and b). It is apparent from the figure that at a very low concentration (10–25 $\mu\text{g ml}^{-1}$) of substrates both P_2 and P_5 exhibit very good cell viability (>90%). On the other hand the 3-arm block copolymer (P_1) (Fig. 10a) has some toxic behaviour (cell viability ~60%) because, the block copolymer have only DMAEMA units at their periphery.⁴⁴ With increasing the concentration of copolymers the cell viability gradually decreases. It is important to note that the cell viability of both the random copolymer (linear and star), however, remains constant at ~78–82% even at a concentration of 200 $\mu\text{g ml}^{-1}$ although at this concentration the cell viability of star block copolymer reduces to the value ~38%. The highly positive surface charged (zeta potential $+28.1 \pm 5.8$ mV) star block copolymer (P_1) shows high cytotoxicity due to significant amount of nonspecific interaction with cells causing increased cellular uptake and hinder cell function compare with the lower positively surface charged linear/star random copolymer (zeta potential $+11 \pm 6.8$ mV for linear & $+13 \pm 7.2$ mV for star random) (Fig. S9†).⁴⁵ For the polymer P_3 which is practically important as a biological material, the cytotoxicity has been tested and this data exhibits 70% cell viability even at 500 $\mu\text{g ml}^{-1}$ concentration (Fig. 10b). In addition, Fig. 11 shows the morphologies of normal CHO-K1 cells in absence and presence of various copolymers to confirm the biocompatibility. The morphology of the cells after 24 hours of incubation at 37 °C in presence of linear and star random copolymers is almost the same with the morphology in absence of polymer indicating

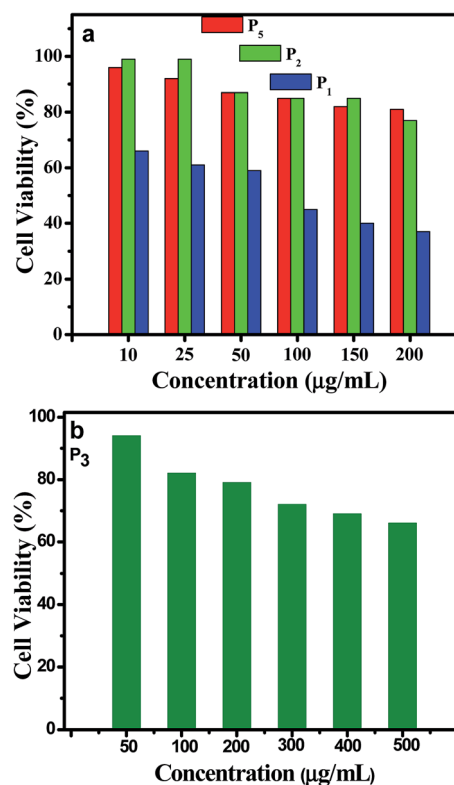


Fig. 10 *In vitro* cytotoxicity of different copolymers in normal CHO-K1 cells after 24 hours incubation at different concentrations.

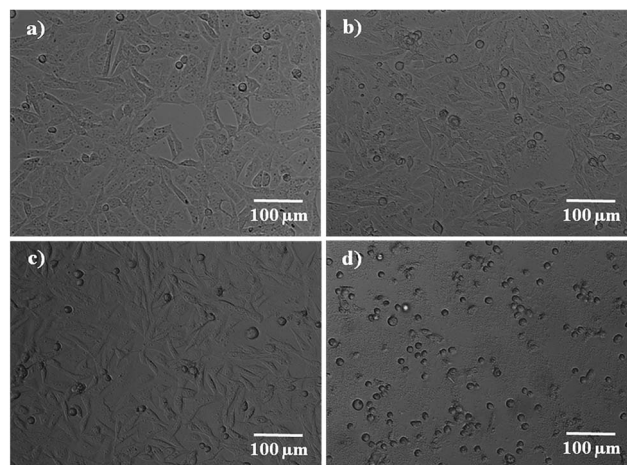


Fig. 11 Differential interference contrast (DIC) images of CHO-K1 cells (a) in absence of copolymer and in presence of (b) P_5 , (c) P_2 and (d) P_1 copolymer after 24 hour incubation in the copolymer solution (200 $\mu\text{g ml}^{-1}$).

good biocompatibility of the polymer. But, the change of morphology of the cells in presence of the star block copolymer (P_1) indicates its prominent toxic effect.

4. Conclusion

ATRP technique is used to synthesise stimuli responsive 3-arm star random/block and linear random copolymers of DEGMA

and DMAEMA. DLS study indicates the self-assembly of these copolymers with increase of temperature at a particular pH due to LCST type phase separation and it persists even in the presence of the fluorescent ANS molecule which enters into the aggregate core of pDEGMA chains. Keeping the temperature fixed if pH is lowered by a small amount the dissociation of the aggregate takes place because of protonation of the basic $-NMe_2$ groups. This is also supported from the fluorescence spectroscopy where the fluorescence intensity of ANS increases due to inclusion in the hydrophobic pDEGMA core and its disaggregation with lowering of pH releases the fluorophores decreasing the PL-intensity. The aggregation and dissociation is highly reversible with respect to the change of temperature and pH. The polymers also exhibit reversible multiple aggregation by triggering temperature and pH. All the co-polymers require increased temperature for aggregation with decreasing pH of the medium. Among all the copolymers, the random copolymer 3-arm-p(DEGMA₄₀-R-DMAEMA₁₈) exhibits aggregation under the physiological conditions and also exhibits good cell viability.

Acknowledgements

We gratefully acknowledge SERB New Delhi (grant no. SB/SI/OC-11/2013) for financial support. S. Das, R. Ghosh and P. Das acknowledges DST "INSPIRE" program and CSIR for providing the fellowship. We acknowledge Dr N. R. Jana of CAM, IACS for helping in MTT assay.

References

- 1 A. V. Dobrynin and M. Rubinstein, *Prog. Polym. Sci.*, 2005, **30**, 1049–1118.
- 2 (a) C. J. F. Rijcken, O. Soga, W. E. Hennink and C. F. van Nostrum, *J. Controlled Release*, 2007, **120**, 131–148; (b) P. De and B. S. Sumerlin, *Macromol. Chem. Phys.*, 2013, **214**, 272–279.
- 3 G. Sukhorukov, A. Fery and H. Mohwald, *Prog. Polym. Sci.*, 2005, **30**, 885–897.
- 4 (a) W. J. Brittain, S. G. Boyes, A. M. Granville, M. Baum, B. K. Mirous, B. Akgun, B. Zhao, C. Bickel and M. D. Foster, *Adv. Polym. Sci.*, 2006, **198**, 125–147; (b) S. G. Roy, K. Bauri, S. Pal and P. De, *Polym. Chem.*, 2014, **5**, 3624–3633.
- 5 (a) E. S. Gil and S. M. Hudson, *Prog. Polym. Sci.*, 2004, **29**, 1173–1222; (b) S. Pal, S. G. Roy and P. De, *Polym. Chem.*, 2014, **5**, 1275–1284.
- 6 (a) Y. Tanaka, J. P. Gong and Y. Osada, *Prog. Polym. Sci.*, 2005, **30**, 1–9; (b) C. de las Heras Alarcon, S. Pennadam and C. Alexander, *Chem. Soc. Rev.*, 2005, **34**, 276–285; (c) A. S. Hoffman, *Adv. Drug Delivery Rev.*, 2013, **6**, 10–16; (d) D. Kuckling and A. Wycisk, *J. Polym. Sci., Part A: Polym. Chem.*, 2013, **51**, 2980–2994; (e) F. Liu and M. W. Urban, *Prog. Polym. Sci.*, 2010, **35**, 3–23; (f) F. D. Jochumab and P. Theato, *Chem. Soc. Rev.*, 2013, **42**, 7468–7483.
- 7 I. Dimitrov, B. Trzebicka, A. H. E. Muller, A. Dworak and C. B. Tsvetanov, *Prog. Polym. Sci.*, 2007, **32**, 1275–1343.
- 8 Y. Jiang, Y. Wang, N. Ma, Z. Wang, M. Smet and X. Zhang, *Langmuir*, 2007, **23**, 4029–4034.
- 9 J. Jiang, X. Tong, D. Morris and Y. Zhao, *Macromolecules*, 2006, **39**, 4633–4640.
- 10 J. Jiang, X. Tong and Y. Zhao, *J. Am. Chem. Soc.*, 2005, **127**, 8290–8291.
- 11 X. Jiang, C. A. Lavender, J. W. Woodcock and B. Zhao, *Macromolecules*, 2008, **41**, 2632–2643.
- 12 H. Lee, W. Wu, J. K. Oh, L. Mueller, G. Sherwood, L. Peteanu, T. Kowalewski and K. Matyjaszewski, *Angew. Chem., Int. Ed.*, 2007, **46**, 2453–2457.
- 13 Y. Katayama, T. Sonoda and M. Maeda, *Macromolecules*, 2001, **34**, 8569–8573.
- 14 J. Joseph, C. A. Dreiss and T. Cosgrove, *Langmuir*, 2007, **23**, 460–466.
- 15 Y. Ishihara, H. S. Bazzi, V. Toader, F. Godin and H. F. Sleiman, *Chem.-Eur. J.*, 2007, **13**, 4560–4570.
- 16 A. Napoli, M. J. Boerakker, N. Tirelli, R. J. M. Nolte, N. A. J. M. Sommerdijk and J. A. Hubbell, *Langmuir*, 2004, **20**, 3487–3491.
- 17 A. Napoli, M. Valentini, N. Tirelli, M. Muller and J. A. Hubbell, *Nat. Mater.*, 2004, **3**, 183–189.
- 18 M. Yamato, Y. Akiyama, J. Kobayashi, J. Yang, A. Kikuchi and T. Okano, *Prog. Polym. Sci.*, 2007, **32**, 1123–1133.
- 19 D. Schmaljohann, *Adv. Drug Delivery Rev.*, 2006, **58**, 1655–1670.
- 20 R. Langer and D. A. Tirrell, *Nature*, 2004, **428**, 487–492.
- 21 (a) A. K. Mishra, N. K. Vishwakarma, V. K. Patel, C. S. Biswas, T. K. Paira, T. K. Mandal, P. Maiti and B. Ray, *Colloid Polym. Sci.*, 2014, **292**, 1405–1418; (b) P. Pramanik and S. Ghosh, *J. Polym. Sci., Part A: Polym. Chem.*, 2015, **53**, 2444–2451.
- 22 J. F. Lutz, O. Akdemir and A. Hoth, *J. Am. Chem. Soc.*, 2006, **128**, 13046–13047.
- 23 T. Pintauer and K. Matyjaszewski, *Coord. Chem. Rev.*, 2005, **249**, 1155–1184.
- 24 K. Matyjaszewski and J. Xia, *Chem. Rev.*, 2001, **101**, 2921–2990.
- 25 J.-F. Lutz, *J. Polym. Sci., Part A: Polym. Chem.*, 2008, **46**, 3459–3470.
- 26 J. F. Lutz and A. Hoth, *Macromolecules*, 2006, **39**, 893–896.
- 27 J. F. Lutz, K. Weichenhan, O. Akdemir and A. Hoth, *Macromolecules*, 2007, **40**, 2503–2508.
- 28 S. Han, M. Hagiwara and T. Ishizone, *Macromolecules*, 2003, **36**, 8312–8319.
- 29 S. Das, S. Samanta, D. P. Chatterjee and A. K. Nandi, *J. Polym. Sci., Part A: Polym. Chem.*, 2013, **51**, 1417–1427.
- 30 S. Das, D. P. Chatterjee, S. Samanta and A. K. Nandi, *RSC Adv.*, 2013, **3**, 17540–17550.
- 31 M. Wang, S. Zou, G. Guerin, L. Shen, K. Deng, M. Jones, G. C. Walker, G. D. Scholes and M. A. Winnik, *Macromolecules*, 2008, **41**, 6993–7002.
- 32 N. Tantavichet, M. D. Pritzker and C. M. Burns, *J. Appl. Polym. Sci.*, 2001, **81**, 1493–1497.
- 33 S. Yamamoto, J. Pietrasik and K. Matyjaszewski, *Macromolecules*, 2008, **41**, 7013–7020.
- 34 X. Jiang and B. Zhao, *Macromolecules*, 2008, **41**, 9366–9375.

- 35 T. G. Olenick, X. Jiang and B. Zhao, *Langmuir*, 2010, **26**, 8787–8796.
- 36 I. F. Tannock and D. Rotin, *Cancer Res.*, 1989, **49**, 4373–4384.
- 37 P. Jie, S. S. Venkatraman, F. Min, B. Y. C. Freddy and G. L. Huat, *J. Controlled Release*, 2005, **110**, 20–33.
- 38 J. Brandrup, E. H. Immergut and E. A. Grulke, *Polymer Handbook*, 4th edn, 1999, pp. VII/2.
- 39 H. J. Jeon, W. J. Jin, E. H. Jeong, J. H. Hong, S. H. Ahn, J. H. Choi, K. S. Cho and J. H. Youk, *Polym. Prepr.*, 2006, **47**, 473–474.
- 40 S. Karanam, H. Goossens, B. Klumperman and P. Lemstra, *Macromolecules*, 2003, **36**, 3051–3060.
- 41 W. A. Braunecker and K. Matyjaszewski, *Prog. Polym. Sci.*, 2007, **32**, 93–146.
- 42 *Hand book of radical polymerization, Control of Free-Radical Polymerization by Chain Transfer Methods*, ed. K. Matyjaszewski, T. P. Davis, J. Chiefari and E. Rizzardo, 2003, p. 680.
- 43 T. K. Georgiou, M. Vamvakaki and C. S. Patrickios, *Biomacromolecules*, 2004, **5**, 2221–2229.
- 44 T. K. Georgiou, M. Vamvakaki, L. A. Phylactou and C. S. Patrickios, *Biomacromolecules*, 2005, **6**, 2990–2997.
- 45 P. Das and N. R. Jana, *ACS Appl. Mater. Interfaces*, 2014, **6**, 4301–4309.